Intrinsic charge transport of conjugated organic molecules in electromigrated nanogap junctions

Hyunwook Song,[1,a)] Youngsang Kim,[2,b)] Heejun Jeong,[2] Mark A. Reed,[3,c)] and Takhee Lee[1,c)]
[1]*Department of Materials Science and Engineering, Department of Nanobio Materials and Electronics, Gwangju Institute of Science and Technology, Gwangju 500-712, Korea*
[2]*Department of Applied Physics, Hanyang University, Ansan 426-791, Korea*
[3]*Departments of Electrical Engineering and Applied Physics, Yale University, New Haven, CT 06520, USA*

(Received 24 July 2010; accepted 28 December 2010; published online 31 May 2011)

We present the measurement of charge transport through phenylene conjugated molecules using electromigrated nanogap junctions. To elucidate the intrinsic transport properties of the conjugated molecular junctions, a variety of molecular transport techniques were performed at low temperature, including inelastic electron tunneling spectroscopy, temperature- and length-variable transport measurements, and transition voltage spectroscopy. Such a self-consistent characterization of the molecular junction demonstrates the observation of intrinsic molecular properties in these junctions. [doi:10.1063/1.3578345]

I. INTRODUCTION

Charge transport through conjugated organic molecules is a field of intense investigation and, until now, a number of different experimental strategies have been exploited in an effort to understand how the molecules transport charge carriers at the single-molecule level.[1–3] Many of these experiments involve connecting the molecules to metal electrodes with a nanometer-sized gap (nanogap). Here we report a study of charge transport characterization of phenylene conjugated molecular series using the electromigrated nanogap junctions. The nanogap fabrication is performed by the controlled passage of a large electrical current through the thin metal wire predefined by electron-beam lithography, causing the electromigration of metal atoms and eventual breakage of the metal wire.[4] In particular, primary focus is made on a coherent tunneling regime, a well-established molecular transport picture where molecular levels remain far above and below the relevant Fermi level of the electrodes, and then the tunneling transport is dominated by the nearest molecular level. In the context of molecular electronics, in which the ultimate aim is to construct the circuitry based on the prescribed electronic function of single molecules, it should be highly desirable to demonstrate intrinsic charge transport through molecular junctions, that is, the transport properties originating from the component molecules, but not other parasitic effects such as impurity-mediated transport.[5,6]

II. EXPERIMENTAL METHODS

The nanogap devices were fabricated by the well-known electromigration technique of fracturing a continuous metal wire.[4] Electron-beam lithography and lift-off are used to create 15 nm-thick Au wires with widths of about 50–100 nm at their narrowest constriction, as shown in Fig. 1(a). After the samples were cleaned in oxygen plasma for 1 min, molecular deposition on the Au surface was performed in a dilute solution (1 mM) of phenylenedithiols in 10 mL ethanol for 24 h, inside a nitrogen-filled glovebox with an oxygen level of < 10 ppm. In this experiment, transport measurements were made on phenylenedithiols with one, two, and three phenyl rings: benzenedithiol (BDT), dibenzenedithiol (DBDT), and tribenzenedithiol (TBDT) molecules. Chemical structures of each molecule are displayed in Fig. 1(b). Before use, each sample was rinsed in ethanol and gently blown dry in a nitrogen stream to remove noncovalently attached molecules.

The electromigration-induced breaking process, and subsequent transport and inelastic electron tunneling spectroscopy (IETS) measurements were carried out at 4.2 K, with a custom-built cryogenic measurement apparatus. The devices (deposited with the molecules as described above) are mounted onto a 28-pin leadless chip carrier socket on the

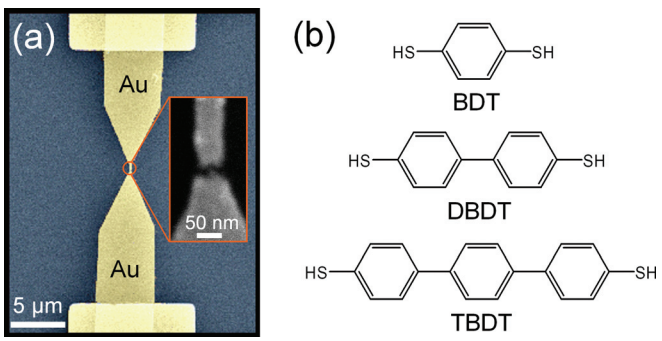

FIG. 1. (Color online) (a) Scanning electron microscopy (SEM) image of continuous Au wire before electromigration. Inset shows SEM image focusing on a broken nanogap after electromigration. (b) Chemical structures of phenylenedithiol molecules used in this study: benzenedithiol (BDT), dibenzenedithiol (DBDT), and tribenzenedithiol (TBDT).

[a)]Present address: Department of Electrical Engineering, Yale University, New Haven, CT 06520, USA.
[b)]Present address: Department of Physics, University of Konstanz, D-78457 Konstanz, Germany.
[c)]Authors to whom correspondence should be addressed. Electronic addresses: tlee@gist.ac.kr (T.L.) or mark.reed@yale.edu (M.A.R.).

sample stage inside a vacuum chamber that is evacuated and purged with He gas before being lowered into a liquid He storage Dewar. The electromigration proceeded to form electrode pairs with a nanometer-scale separation by ramping up a dc voltage as shown in the inset of Fig. 1(a), across which the molecules are occasionally attached. The electromigrated break junctions have potentially been regarded as a single or very few molecules junction.[4] To measure the current (I)−voltage (V) characteristics, we used a 16-bit digital-to-analog converter for bias voltages, and a low-noise current amplifier (Ithaco 1211) followed by a digital multimeter (Agilent 34 410) for current measurement. The IETS (d^2I/dV^2) spectrum was directly measured using a lock-in amplifier (Stanford Research Systems 830) and a homebuilt current−voltage sweeper controlled by a computer running via GPIB. An ac modulation of 7.8 mV (root-mean-square) at a frequency of 1033 Hz with a lock-in time constant of 1 s was applied to the sample to obtain the second harmonic signals, proportional to d^2I/dV^2.

III. RESULTS AND DISCUSSION

In this study, we have focused on the devices showing reproducible symmetry $I(V)$ curves with a sigmoid shape,[7] indicating a typical coherent tunneling feature of a molecular junction with strong molecule−electrodes coupling.[8–10] In what follows, we show the molecular contribution to charge transport in these junctions by performing a variety of molecular transport techniques. The yield of devices that indicate molecular effects (see discussion below) was ~5%.

The temperature-variable $I(V)$ measurement is necessary to examine the charge transport mechanism for molecular junctions.[11,12] Figure 2 shows a representative temperature-variable $I(V)$ characteristic of Au−BDT−Au junctions measured using the aforementioned nanogap device structures. The $I(V)$ curves were measured between 4.2 and 90 K, and no temperature dependence was observed. The temperature-independent $I(V)$ behavior is a clear manifestation of tunneling, and eliminates many other potential alternative mechanisms such as thermionic emission or hopping conduction. The tunneling transport can also be verified by examining the dependence of conductance on the molecular length.[11–15] For nonresonant tunneling, the conductance (G) will show an exponential decrease as the molecular length increases according to Eq. (1)

$$G \sim \exp(-\beta d), \tag{1}$$

where d is the molecular length and β is the tunneling decay coefficient. Other length dependencies of conductance are possible, indicative of alternative transport mechanisms; for example, the conductance is expected to scale linearly with the molecular length in the case of hopping conduction.[12] In Fig. 3(a), we examined the length-dependent conductance with three different phenylenedithiols, that is, BDT, DBDT, and TBDT. The conductance values were obtained by

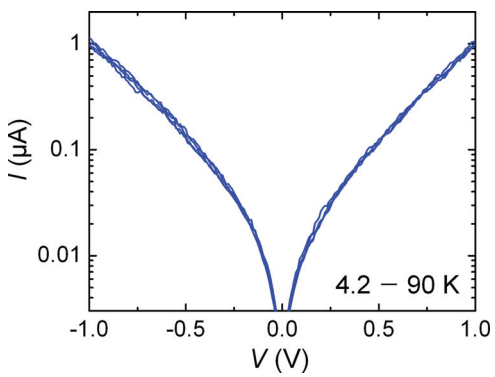

FIG. 2. (Color online) Semilog plot of temperature-variable $I(V)$ characteristics for Au−BDT−Au junctions at selected temperatures (4.2, 30, 60, and 90 K).

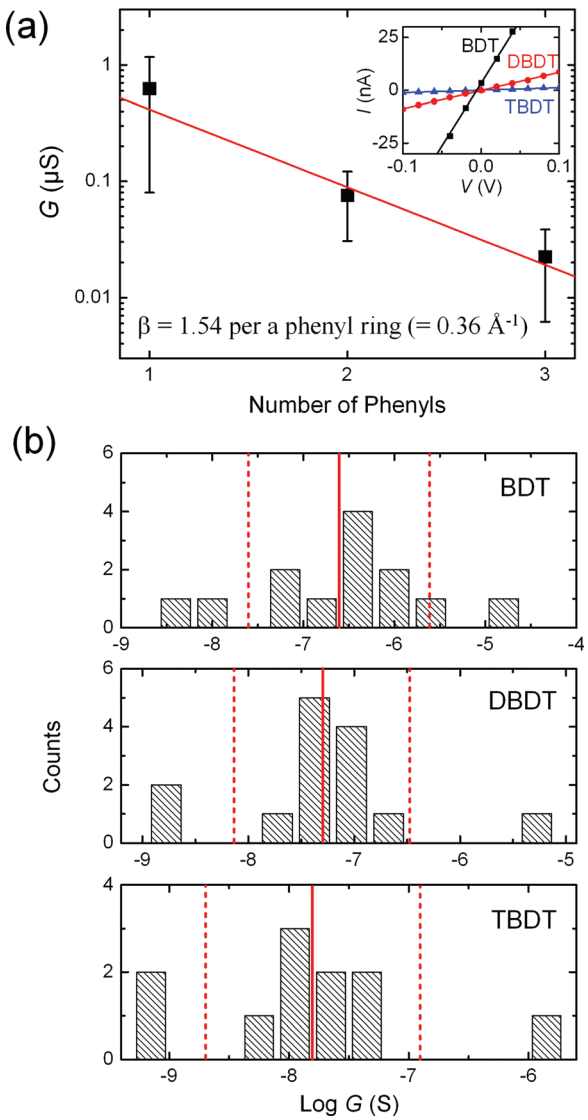

FIG. 3. (Color online) Semilog plot of the conductance vs the number of phenyls. The decay coefficient (β) can be determined from the linear fit according to Eq. (1), yielding a β value of 1.54 per phenyl ring (=0.36 $Å^{-1}$). Inset shows length-dependent $I(V)$ curves in the low-bias linear regime, where a conductance value is obtained from linear fits to the data. (b) Statistical histograms of the conductance values measured for BDT, DBDT, and TBDT. The vertically dashed line and solid line represent the mean value (m) and standard deviation (σ), respectively. Data outside the range between $m+\sigma$ and $m-\sigma$ (the range between vertically dashed lines) in the logarithmic histograms are excluded in the plot of (a). Then, the β value is determined only using the data within the vertically dashed lines (i.e., by applying the one σ criteria).

performing least-squares linear fit from low-bias regimes ($-0.1\ \text{V} \le V \le 0.1\ \text{V}$) of $I(V)$ curves, as shown in the inset of Fig. 3(a). Figure 3(b) shows statistical histograms for the conductance values. In the logarithmic histograms, the data only within the standard deviation (σ; dashed lines) for the mean value (m; solid lines) (i.e., in the range between $m+\sigma$ and $m-\sigma$) are used to generate Fig. 3(a) (and thus to obtain a β value; see below). In accordance with Eq. (1), Fig. 3(a) shows that a semilog plot of the conductance values versus the molecular length (the number of phenyls) is linear, in which each data point represents the average of data selected with the one σ criteria as described above, and the error bars are the standard deviation for the selected data. We found a β value of 1.54 per phenyl ring ($=0.36\ \text{Å}^{-1}$) from the linear fit in Fig. 3(a). This β value is in good agreement with the previously reported values for a series of oligophenylenes in literature.[3,15] Indeed, a nonresonant tunneling mechanism for the short-length molecules of phenylenedithiols or other conjugated series has been extensively confirmed in various testbeds for molecular transport experiments,[3,12,15] indicating that the Fermi level of the electrode lies deep within their highest occupied molecular orbital (HOMO)-lowest unoccupied molecular orbital (LUMO) gap, and thus a considerable energy barrier against transporting charge carriers across the molecular junction is created.

Inelastic electron tunneling spectroscopy (IETS) has been introduced as a primary tool for identification of the component molecules present in molecular junctions,[16–19] analogous to infrared and Raman spectroscopy for macroscopic samples. In IETS, an inelastic tunneling channel is open, in addition to the elastic one, above the excitation threshold $|eV| = \Omega$ for a molecular vibration (where e is elementary charge, V is applied bias, and Ω is vibrational energy).[20] The conductance change caused by the opening of the inelastic channel at $|eV| = \Omega$ can be clearly observed as reproducible features (usually peaks) in the second derivative d^2I/dV^2 plotted against V.[20] Figure 4 shows a representative IETS spectrum of Au-BDT-Au junctions. A standard ac modulation technique with a lock-in amplifier was carried out at 4.2 K to directly acquire the second (d^2I/dV^2) harmonic signals. The spectra are stable and reproducible upon successive bias sweep, and the same vibrational peaks are observed repetitively for other BDT junctions. We assign the observed spectral features to specific molecular vibrations by comparison with previously reported infrared, Raman, and IETS measurements, and also by density functional theory calculations. In the IETS spectrum of the BDT junction, three prominent peaks reproducibly appear at 96, 142, and 201 mV, which correspond to γ(C-H) aryl out-of-plane bending, ν(18a) stretching, and ν(8a) stretching modes, respectively. These modes originate from vibrations of the phenyl ring. A theoretical study predicted that the ν(18a) and ν(8a) ring modes should have the strong vibronic coupling in phenylene molecules,[21] and is consistent with our results. Also, the dominance of aromatic ring modes in IETS spectra has been experimentally observed for various conjugated molecules.[17,22] The fully assigned IETS spectrum provides an unambiguous experimental evidence of the existence of the desired molecules in the junction, without anything else. Taken together with the tunneling dependencies, this suggests that the IETS-identified molecule is the only thing in the junction through which tunneling is occurring.

Transition voltage spectroscopy (TVS) has recently become a popular method as a spectroscopic tool for molecular junctions[19,23–25] and other diverse nanoelectronic systems.[26–28] Specifically, TVS is used to give insight into the energy offset between the contact Fermi level and the nearest molecular level responsible for charge transport in molecular junctions by measuring a transition voltage (V_{trans}) required to generate inflection behavior of a Fowler–Nordheim plot, the corresponding analysis of $\ln(I/V^2)$ against $1/V$ for $I(V)$ characteristics. Figure 5 shows the measurement of V_{trans} for BDT, DBDT, and TBDT. To make Fig. 5, representative

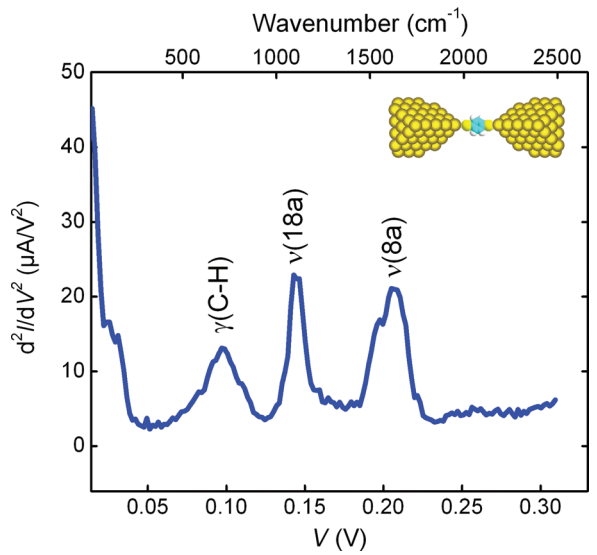

FIG. 4. (Color online) IETS spectrum (d^2I/dV^2) of Au–BDT–Au junctions, directly obtained from lock-in second harmonic signal at 4.2 K. The peaks are labeled with their assigned vibrational modes, given in terms of Wilson–Varsanyi terminology (Ref. 30). Inset shows a schematic of the Au–BDT–Au structure incorporated into the electromigrated nanogap junctions.

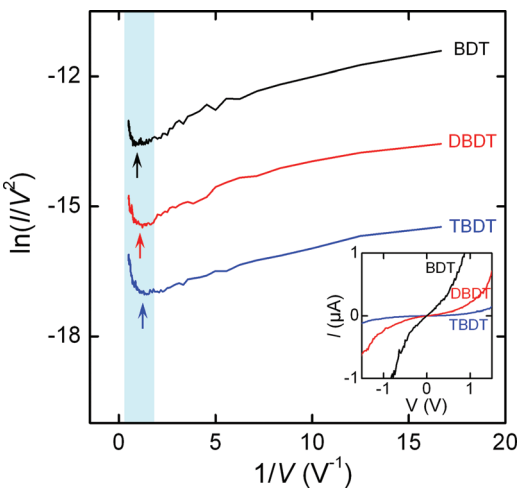

FIG. 5. (Color online) $\ln(I/V^2)$ vs $1/V$ plots for BDT, DBDT, and TBDT, where the arrows denote transition voltage (V_{trans}). Inset shows corresponding $I(V)$ curves. All data were obtained at 4.2 K.

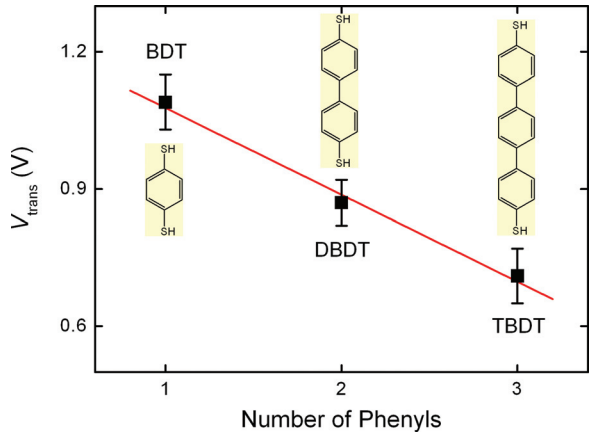

FIG. 6. (Color online) Plot of V_{trans} as a function of the number of phenyl rings for phenylenedithiols. The solid line is a linear fit to the three data points. Error bars on each data point also represent the standard deviation across individual measurements for different devices. Chemical structures for each molecule are also shown in the inset.

$I(V)$ curves of each molecule in the inset of Fig. 5 were transformed to axes of $\ln(I/V^2)$ against $1/V$, in which an inflection point denotes V_{trans} (as indicated by the arrow). V_{trans} for phenylenedithiols is summarized graphically in Fig. 6. Our TVS measurements explicitly show that V_{trans} decreases with molecular length for phenylenedithiols. In general, the HOMO-LUMO gap of π-conjugated molecules is known to decrease with an increase in conjugation length.[29] It is thus reasonable to expect longer conjugated molecules to exhibit a smaller value of V_{trans} than shorter conjugated molecules within a given molecular series. Beebe *et al.* previously showed that V_{trans} decreases with the increasing molecular length of conjugated molecules,[24] as well as a decrease in the energy offset between the contact Fermi level and the nearest molecular level with extending conjugation, determined by ultraviolet photoelectron spectroscopy measurements.[23] Our electromigrated-gap TVS measurements are consistent with these results, providing additional verification of this technique for probing intrinsic molecular properties in these conjugated molecular junctions.

IV. CONCLUSIONS

We have demonstrated intrinsic charge transport properties of phenylene conjugated molecules employing the electromigrated nanogap junctions. The temperature-independent $I(V)$ characteristics and the exponential decay of conductance with molecular length indicate that nonresonant tunneling is a dominant charge transport mechanism for the short-length conjugated molecules. We have also shown the completely assigned IETS spectrum in which all of the spectral features are attributable to vibrational modes associated with the molecular species. Moreover, TVS measurements for the phenylene series have shown that V_{trans} decreases with extending conjugation length, which is consistent with a decrease in energy offset between the contact Fermi level and the nearest molecular level with extent of delocalization across conjugated molecules.

ACKNOWLEDGMENTS

This work was supported by the Korean National Research Laboratory program, a Korean National Core Research Center grant, the World Class University program of the Korean Ministry of Education, Science and Technology of Korea, the Program for Integrated Molecular System at the Gwangju Institute of Science and Technology, the US Army Research Office (W911NF-08-1-0365), and the Canadian Institute for Advanced Research (CIfAR).

[1] M. A. Reed and T. Lee, *Molecular Nanoelectronics* (American Scientific, Stevenson Ranch, 2003).
[2] G. Cuniberti, G. Fagas, and K. Richter, *Introducing Molecular Electronics* (Springer-Verlag, Berlin, 2005).
[3] N. J. Tao, Nat. Nanotechnol. **1**, 173 (2006).
[4] H. Park, A. K. L. Lim, A. P. Alivisatos, J. Park, and P. L. McEuen, Appl. Phys. Lett. **75**, 301 (1999).
[5] A. A. Houck, J. Labaziewicz, E. K. Chan, J. A. Folk, and I. L. Chuang, Nano Lett. **5**, 1685 (2005).
[6] K. Luo, D. H. Chae, and Z. Yao, Nanotechnology **18**, 465203 (2007).
[7] Other transport characteristics were also observed; for example, Coulomb blockade, zero-bias enhancement of conductance, asymmetry $I(V)$ curves, and current-induced irreversible changes in $I(V)$ curves. We excluded these devices in the present study. A variety of $I(V)$ characteristics are caused by the microscopic differences in the nanogap structure, molecule−electrodes interface, molecular arrangement, presence of metal debris or unintentional impurities in the gap, and so on. In addition, temperature-induced irreversible devices were also excluded in this study, which are likely caused by a change in gap widths with the temperature variation.
[8] S. Ghosh, H. Halimun, A. K. Mahapatro, J. Choi, S. Lodha, and D. Janes, Appl. Phys. Lett. **87**, 233509 (2005).
[9] Y. Selzer, M. A. Cabassi, T. S. Mayer, and D. L. Allara, J. Am. Chem. Soc. **126**, 4052 (2004).
[10] Y. Selzer, L. Cai, M. A. Cabassi, Y. Yao, J. M. Tour, T. S. Mayer, and D. L. Allara, Nano Lett. **5**, 61 (2005).
[11] W. Wang, T. Lee, and M. A. Reed, Phys. Rev. B **68**, 035416 (2003).
[12] S. H. Choi, B. Kim, and C. D. Frisbie, Science **320**, 1482 (2008).
[13] R. E. Holmlin, R. Haag, M. L. Chabinyc, R. F. Ismagilov, A. E. Cohen, A. Terfort, M. A. Rampi, and G. M. Whitesides, J. Am. Chem. Soc. **123**, 5075 (2001).
[14] D. J. Wold and C. D. Frisbie, J. Am. Chem. Soc. **123**, 5549 (2001).
[15] D. J. Wold, R. Haag, M. A. Rampi, and C. D. Frisbie, J. Phys. Chem. B **106**, 2813 (2002).
[16] W. Wang, T. Lee, I. Kretzschmar, and M. A. Reed, Nano Lett. **4**, 643 (2004).
[17] J. G. Kushmerick, J. Lazorcik, C. H. Patterson, R. Shashidhar, D. S. Seferos, and G. C. Bazan, Nano Lett. **4**, 639 (2004).
[18] M. Galperin, M. A. Ratner, A. Nitzan, and A. Troisi, Science **319**, 1056 (2008).
[19] H. Song, Y. Kim, Y. H. Jang, H. Jeong, M. A. Reed, and T. Lee, Nature (London) **462**, 1039 (2009).
[20] R. C. Jaklevic and J. Lambe, Phys. Rev. Lett. **17**, 1139 (1966).
[21] A. Troisi, M. A. Ratner, and A. Nitzan, J. Chem. Phys. **118**, 6072 (2003).
[22] D. P. Long, J. L. Lazorcik, B. A. Mantooth, M. H. Moore, M. A. Ratner, A. Troisi, Y. Yao, J. W. Ciszek, J. M. Tour, and R. Shashidhar, Nature Mater. **5**, 901 (2006).
[23] J. M. Beebe, B. Kim, J. W. Gadzuk, C. D. Frisbie, and J. G. Kushmerick, Phys. Rev. Lett. **97**, 026801 (2006).
[24] J. M. Beebe, B. Kim, C. D. Frisbie, and J. G. Kushmerick, ACS Nano **2**, 827 (2008).
[25] E. H. Huisman, C. M. Guédon, B. J. van Wees, and S. J. van der Molen, Nano Lett. **9**, 3909 (2009).
[26] S. A. DiBenedetto, A. Facchetti, M. A. Ratner, and T. J. Marks, J. Am. Chem. Soc. **131**, 7158 (2009).
[27] M. Choe, G. Jo, J. Maeng, W. K. Hong, M. Jo, G. Wang, W. Park, B. Lee, H. Hwang, and T. Lee, J. Appl. Phys. **107**, 034504 (2010).
[28] P. W. Chiu and S. Roth, Appl. Phys. Lett. **92**, 042107 (2008).
[29] L. O'Neill and H. J. Byrne, J. Phys. Chem. B **109**, 12685 (2005).
[30] G. Varsanyi, *Assignments for Vibrational Spectra of Seven Hundred Benzene Derivatives* (Wiley, New York, 1974).